

## Communication

<sup>14</sup>N Polarization Inversion Spin Exchange at Magic Angle (PISEMA)

Chunqi Qian, Riqiang Fu, Peter Gor'kov, William W. Brey, Timothy A. Cross, Zhehong Gan \*

Center for Interdisciplinary Magnetic Resonance, National High Magnetic Field Laboratory, 1800 E. Paul Dirac Drive, Tallahassee, FL 32310, USA

## ARTICLE INFO

## Article history:

Received 20 August 2008

Revised 10 October 2008

Available online 17 October 2008

## Keywords:

Nitrogen

N-14 PISEMA

Dipolar coupling

Quadrupolar coupling

Spin-exchange

Oriented sample

Membrane protein

## ABSTRACT

Polarization Inversion Spin Exchange at Magic Angle (PISEMA) is a powerful experiment for determining peptide orientation in uniformly aligned samples such as planar membranes. In this paper, we present <sup>14</sup>N-PISEMA experiment which correlates <sup>14</sup>N quadrupolar coupling and <sup>14</sup>N–<sup>1</sup>H dipolar coupling. <sup>14</sup>N-PISEMA enables the use of <sup>14</sup>N quadrupolar coupling tensor as an ultra sensitive probe for peptide orientation and can be carried out without the need of isotope enrichment. The experiment is based on selective spin-exchange between a proton and a single-quantum transition of <sup>14</sup>N spins. The spin-exchange dynamics is described and the experiment is demonstrated with a natural abundant *N*-acetyl valine crystal sample.

© 2008 Elsevier Inc. All rights reserved.

## 1. Introduction

Nitrogen is one of the most important elements in biological chemistry. Traditionally, nitrogen NMR spectroscopy has relied exclusively on observing <sup>15</sup>N either at 0.37% natural abundance or with isotope labeling for favorable NMR properties of spin-1/2. Despite of high natural abundance (99.6%) <sup>14</sup>N NMR has been rare due to the low gyromagnetic ratio and large quadrupolar interactions of the spin-1 nucleus. Nevertheless <sup>14</sup>N NMR is capable of accessing quadrupolar interaction and measuring electric-field-gradient (EFG) parameters of nitrogen [1–7]. The spectroscopic difficulties of wide-line <sup>14</sup>N NMR can be partially overcome by indirect detection through more sensitive spins like <sup>13</sup>C or <sup>1</sup>H under magic-angle spinning condition of powder samples [8–12]. For single crystal and oriented samples such as peptide and proteins in membranes, large <sup>14</sup>N quadrupolar couplings cause only peak splitting. The presence of quadrupolar interaction does not contribute to the line broadening and the associated problems of low sensitivity and resolution. The measurement of quadrupolar splitting provides the information on molecular orientation of the quadrupolar coupling tensor relative to the magnetic field direction. The orientation approach for structural determination becomes more powerful in the form of multi-dimensional experiments that separate the anisotropic chemical shielding, dipolar and quadrupolar interactions along various dimensions [13,14]. The most notable is the Polarization Inversion Spin Exchange at Magic Angle (PISEMA) experiment [15] which correlates

<sup>15</sup>N chemical shift with <sup>15</sup>N–<sup>1</sup>H dipolar coupling. The two-dimensional <sup>14</sup>N–<sup>1</sup>H Separated-Local-Field (SLF) experiment is another example that utilizes the <sup>14</sup>N quadrupolar interaction [16]. In this paper, we present <sup>14</sup>N Polarization Inversion Spin Exchange at Magic Angle (PISEMA) experiment which has enhanced dipolar resolution over the traditional 2D SLF experiment. [17].

The PISEMA experiment measures the spin-exchange driven by the flip-flop dipolar Hamiltonian. Flip-flop Hamiltonians among various spin pairs do not commute, therefore the largest coupling of the strongly coupled spin pair suppresses the spin-exchange of other weakly coupled ones, namely dipolar truncation. The dipolar truncation often causes problems in polarization transfer to long-range weakly coupled spins [18], but the effect works favorably in PISEMA because it eliminates dipolar broadening effect from the surrounding protons of a <sup>15</sup>N–<sup>1</sup>H spin pair [19]. The resulting line narrowing dramatically enhances the dipolar resolution and has made <sup>15</sup>N–<sup>1</sup>H PISEMA the experiment of choice for determining peptide orientation. The <sup>14</sup>N experiment described here keeps the high dipolar resolution feature of PISEMA and uses the large amide <sup>14</sup>N quadrupolar coupling tensor as one of the orientation probe. Further more, the high <sup>14</sup>N natural abundance makes the experiment applicable to bio-molecules without the need of isotope enrichment.

Spin-exchange in the rotating frame requires spin-lock. For <sup>14</sup>N, the *rf* field is usually not strong enough compared to the quadrupolar interaction for simultaneous spin-lock of both single-quantum transitions. It will be shown here that in most cases that the quadrupolar frequency is much larger than  $\omega_1 = \gamma B_1$  the three-level system of spin-1 can be simplified to a two-level system and selective spin-lock of one single-quantum transition can be achieved.

\* Corresponding author. Fax: +1 850 644 1366.

E-mail address: [gan@magnet.fsu.edu](mailto:gan@magnet.fsu.edu) (Z. Gan).

Cross-polarization and spin-exchange to the selected transition can occur similarly with a spin-1/2 system for obtaining  $^{14}\text{N}$ - $^1\text{H}$  PISEMA spectra.

## 2. Theory

In the rotating frame of the  $rf$  field, the  $^{14}\text{N}$  Hamiltonian consists of the first-order quadrupolar coupling  $\omega_Q(S_z^2 - S^2/3)$  and an offset term  $\Delta\omega_0 S_z$  relative to the Larmor frequency. The offset  $\Delta\omega_0$  includes the contributions from the chemical shift and the second-order quadrupolar shift that both are proportional to  $S_z$ . The Hamiltonian can be expressed explicitly in the three-by-three matrix representation of spin-1.

$$H_N = \omega_Q(S_z^2 - S^2/3) + \Delta\omega_0 S_z = \begin{pmatrix} \Delta\omega_0 + \frac{\omega_Q}{3} & & \\ & -\frac{2\omega_Q}{3} & \\ & & -\Delta\omega_0 + \frac{\omega_Q}{3} \end{pmatrix} \quad (1)$$

Similarly for the  $^{14}\text{N}$ - $^1\text{H}$  dipolar Hamiltonian and the  $rf$  Hamiltonian, we have

$$H_D = \omega_D S_z I_z = \omega_D \begin{pmatrix} 1 & & \\ & 0 & \\ & & -1 \end{pmatrix} \otimes I_z \quad (2)$$

$$H_{rf} = \omega_{1N} S_x + \omega_{1H} I_x = \frac{\omega_{1N}}{\sqrt{2}} \begin{pmatrix} 0 & 1 & 0 \\ 1 & 0 & 1 \\ 0 & 1 & 0 \end{pmatrix} + \omega_{1H} I_x \quad (3)$$

Usually the  $^{14}\text{N}$  quadrupolar interaction is much larger than the  $rf$  Hamiltonian  $|\omega_Q| \gg \omega_{1N}$ . The  $rf$  field is selective to one of two single-quantum transitions with  $\Delta\omega_0 \sim \omega_Q$  or  $-\omega_Q$ . Therefore the three-level  $^{14}\text{N}$  spin system can be simplified to a two-level system described by single-transition  $s = 1/2$  spin operators. Under the two-level approximation, the  $rf$  Hamiltonian becomes

$$H_{rf} = \frac{\omega_{1N}}{\sqrt{2}} \begin{pmatrix} 0 & 1 \\ 1 & 0 \end{pmatrix} + \omega_{1H} I_x = \sqrt{2}\omega_{1N} S_x + \omega_{1H} I_x \quad (4)$$

The  $^{14}\text{N}$  nutation frequency for selective  $rf$  irradiation equals to  $\sqrt{2}$  times  $\gamma B_1$ . This scaling factor needs be considered in the Hartman-Hahn match for the cross-polarization and spin-exchange.

For the quadrupolar and dipolar Hamiltonian, there is an intriguing effect from the two-level approximation. Let us first consider selective  $rf$  field to  $|1\rangle \leftrightarrow |0\rangle$  transition ( $\Delta\omega_0 \sim -\omega_Q$ ). An identity term arises from the two-level spin-1/2 approximation.

$$H_N = \begin{pmatrix} \Delta\omega_0 + \omega_Q/3 & \\ & -2\omega_Q/3 \end{pmatrix} = \left(\frac{\Delta\omega_0}{2} - \frac{\omega_Q}{6}\right) \begin{pmatrix} 1 & 0 \\ 0 & 1 \end{pmatrix} + (\Delta\omega_0 + \omega_Q) \begin{pmatrix} 1/2 & 0 \\ 0 & -1/2 \end{pmatrix} = \left(\frac{\Delta\omega_0}{2} - \frac{\omega_Q}{6}\right) \hat{e} + \omega_{off} S_z \quad (5)$$

Here we use  $\omega_{off} = \Delta\omega_0 + \omega_Q$  to describe the frequency offset to the selectively observed transition. The identity  $\hat{e}$  term in the quadrupolar Hamiltonian has no effect on the spin dynamics. However, the identity term manifests itself into a proton shift in the dipolar Hamiltonian

$$H_D = \omega_D \begin{pmatrix} 1 & \\ & 0 \end{pmatrix} \otimes I_z = \omega_D S_z I_z + \frac{1}{2} \omega_D I_z \quad (6)$$

The shift term  $\frac{1}{2} \omega_D I_z$  changes its sign for the other single-quantum transition  $|0\rangle \leftrightarrow |-1\rangle$  transition ( $\Delta\omega_0 \sim \omega_Q$ ).

$$H_D = \omega_D \begin{pmatrix} 0 & \\ & -1 \end{pmatrix} \otimes I_z = \omega_D S_z I_z - \frac{1}{2} \omega_D I_z \quad (7)$$

This shift term can be visualized in the proton triplet spectrum split by the dipolar coupling from the  $S = 1$   $^{14}\text{N}$  spin [20]. When the two-level approximation is applied to just one of the  $^{14}\text{N}$  single-quantum transition, the average position of the two adjacent peaks in the triplet proton spectrum is shifted off the center by  $\omega_D/2$ , similar to a change of chemical shift. The sign of this shift is opposite between the two single-quantum  $^{14}\text{N}$  transitions.

Eqs. (4)–(7) show that the Hamiltonians under two-level approximation are nearly identical to those of spin-1/2 PISEMA except two differences: First, the  $^{14}\text{N}$  nutation frequency is scaled up by  $\sqrt{2}$ . Second, the identity term in the dipolar Hamiltonian contributes as additional proton chemical and can have effects on the proton decoupling and the spin-exchange. Besides these two differences, the spin dynamics of spin-lock and exchange is the same as spin-1/2 PISEMA. Therefore  $^{14}\text{N}$ -PISEMA spectra can be obtained as long as the  $^{14}\text{N}$   $rf$  irradiation is kept selective  $|\omega_Q| \gg \omega_{1N}$ . When the quadrupolar frequency becomes comparable to  $\omega_{1N}$ , the two-level approximation is invalid. The  $^{14}\text{N}$   $rf$  nutation becomes complicated for the three-level system affecting the dipolar oscillation of the spin-exchange.

## 3. Results and discussion

All experiments were performed on a Bruker Avance-600 MHz spectrometer equipped with a double resonance  $low-E$  probe developed at the NHMFL [21]. The following procedure was used to search for  $^{14}\text{N}$  peaks spanning over several megahertz using cross-polarization. First, proton and  $^{14}\text{N}$   $rf$  fields were calibrated using an  $\text{NH}_4\text{Cl}$  powder sample which has almost zero quadrupolar and dipolar couplings due to the high symmetry and rotational mobility of the ammonium ion. Second, glycine powder sample was used to optimize the cross-polarization condition. The  $^{14}\text{N}$  carrier frequency was set to  $\sim 300$  kHz away from its Larmor frequency to fulfill the two-level approximation. The  $\sqrt{2}$  factor to the  $^{14}\text{N}$  nutation frequency needs be considered for matching the Hartman-Hahn condition with the calibrated proton and  $^{14}\text{N}$   $rf$  fields of  $\gamma B_1/2\pi = 50$  kHz and 35 kHz, respectively. For powder samples, only a fraction of the molecules falls within the effective cross-polarization bandwidth. The signal from  $\sim 50$  kHz bandwidth was sufficiently strong for glycine after 12 scans. The 50 kHz bandwidth was also used as the frequency increment in search for the  $^{14}\text{N}$  signal of the  $N$ -acetyl-D-valine single crystal sample.

The  $N$ -acetyl-D-valine single crystal was grown out of a saturated water solution and has a cubic edge length of 2.5 mm. A total of eight resonance lines were found within a  $\pm 1$  MHz window from the Larmor frequency. Individual  $^{14}\text{N}$  PISEMA experiments were performed on each of these resonance frequencies. The PISEMA pulse sequence is the same as that of  $^{15}\text{N}$  except the  $^{14}\text{N}$   $rf$  field strength (Fig. 1). In addition, the proton frequency offset was calibrated for optimal decoupling by finding the most effective continuous wave decoupling.

Fig. 1 shows the pulse sequence and composed  $^{14}\text{N}$  PISEMA spectra of  $N$ -acetyl-D-valine. There are altogether four pairs of peaks along the F2 dimension split by the  $^{14}\text{N}$  quadrupolar coupling with the frequencies summarized in Table I. The line width ranges from 600 to 700 Hz. The peaks spread nearly 2 MHz as the results of different orientation of the  $^{14}\text{N}$  quadrupolar coupling tensor relative to the magnetic field. The dipolar splitting for the three outer pairs,  $F_2 = (765.0, -711.0)$ ,  $(704.9, -649.1)$  and  $(571.6, -520.5)$  kHz are 14.2, 14.4 and 5.9 kHz, respectively. The dipolar spectra for the  $(136.8, -85.0)$  kHz pair are broad mostly due to the break down of two-level approximation with the quadrupolar frequency being the closest to the  $^{14}\text{N}$  nutation frequency.

It should be noted that the pairs of  $^{14}\text{N}$  peaks split by the quadrupolar couplings are not exact symmetric. The mean frequency

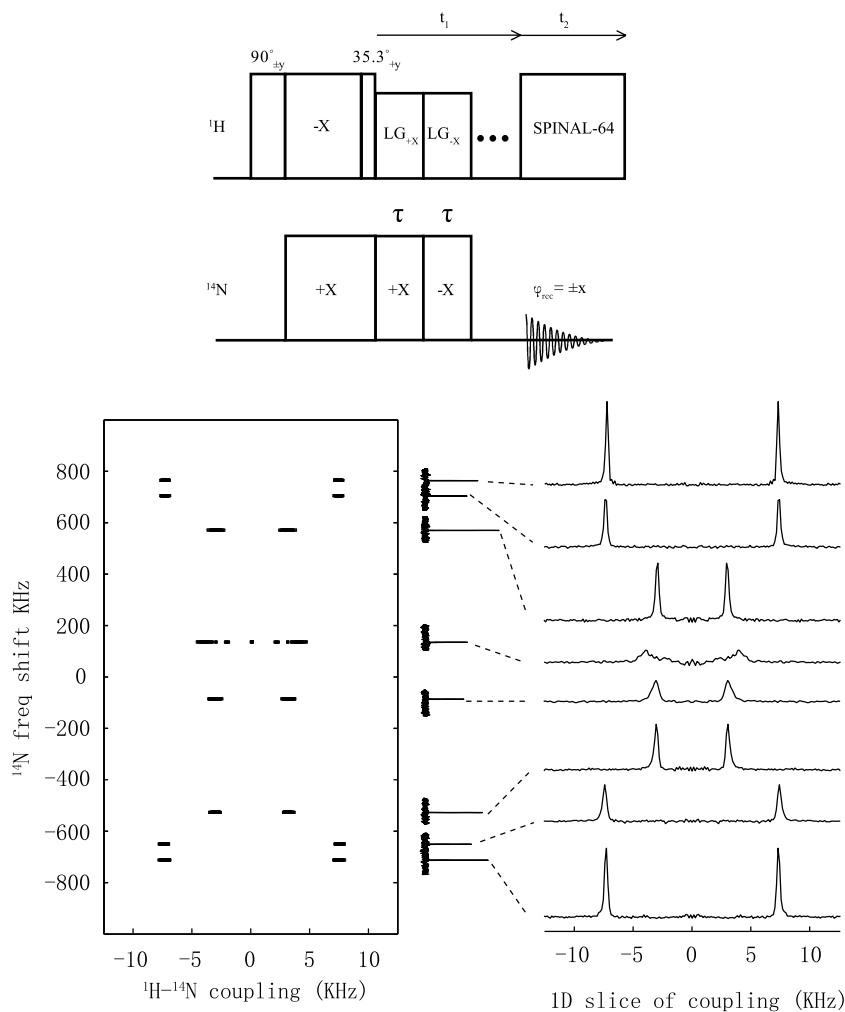


**Fig. 1.**  $^{14}\text{N}$ -PISEMA pulse sequence and composed spectra of *N*-acetyl-D-valine single crystal at an arbitrary orientation. The 1D slices show the dipolar  $^{14}\text{N}$ - $^1\text{H}$  spectra. The F1 axis is scaled by 0.816 for PISEMA. The spectra were acquired using a Bruker Avance-600MHz spectrometer equipped with a double resonance low-E probe developed at the NHMFL [21]. The  $t_1$  increment corresponds to two Lee-Goldburg cycles  $2\tau$  of 40  $\mu\text{s}$ . A total of 128  $t_1$  increment with 8 scans each and 3 s recycle delay were collected for each spectrum.

**Table 1**

Summary of  $^{14}\text{N}$  peak frequencies,  $^1\text{H}$  carrier frequency for optimal  $^1\text{H}$  decoupling,  $^{14}\text{N}$  quadrupolar and  $^{14}\text{N}$ - $^1\text{H}$  dipolar splitting in kHz for four pairs of quadrupolar split peaks of a *N*-acetyl-D-valine crystal at an arbitrary orientation. The  $^{14}\text{N}$  and  $^1\text{H}$  frequency offsets are calibrated with  $\text{NH}_4\text{Cl}$  and  $\text{H}_2\text{O}$ , respectively.

$\nu_{\text{N}}^+$	$\nu_{\text{H}}^+$	$\nu_{\text{N}}^-$	$\nu_{\text{H}}^-$	$(\nu_{\text{N}}^+ + \nu_{\text{N}}^-)/2$	$\nu_{\text{Q}}$	$\nu_{\text{D}}$	$\nu_{\text{H}}^+ - \nu_{\text{H}}^-$
765.0	-7.8	-711.0	5.4	27.0	623 ppm	1476	14.2
704.9	-7.8	-649.1	5.4	27.9	644 ppm	1354	14.4
571.6	-2.1	-520.5	2.7	25.6	590 ppm	1092.1	5.9
136.8	-2.1	-85.0	2.7	25.9	598 ppm	221.8	N/A

deviates from the Larmor frequency as the results of chemical and second-order quadrupolar shifts. A rough estimate here shows that the orientation-independent isotropic parts of the two shifts account for most of the observed frequency deviations. For amide nitrogen, the isotropic second-order quadrupolar shift is about 500 ppm at 14.1 T ( $\sim 21.7$  kHz down field at 600 MHz magnet) [9]. The isotropic chemical shift of amide nitrogen adds another  $\sim 110$  ppm [22]. The isotropic portion of the two shifts adds up to about 610 ppm or 26 kHz, very close the mean frequencies of all four pairs of  $^{14}\text{N}$  peaks ranging from 25.6 to 27.9 kHz down field.

For each pair of  $^{14}\text{N}$  peaks, the frequency for optimal proton decoupling was found different. As mentioned previously Eqs. (6) and (7), this difference comes from the identity term arising from the two-level approximation in the  $^{14}\text{N}$ - $^1\text{H}$  dipolar Hamiltonian. From the calibrations, a 13.2 kHz frequency difference was found for the  $^{14}\text{N}$  pairs at (765.0, -711.0), (704.9, -649.1) kHz, and a 4.8 kHz difference was found for the pair at (571.6, -520.5) kHz. These frequency differences agree qualitatively with the dipolar splitting (14.2, 14.4 and 5.9 kHz) as expected from the theory.

The dipolar spectra of PISEMA are intrinsically symmetric therefore are unable to distinguish the sign of dipolar coupling. The dipolar-induced proton shift can help in the sign determination which can remove some ambiguities in structural refinement using orientation constraints [23]. Eq. [5] and [6] show that the product of  $^{14}\text{N}$  quadrupolar shift and the dipolar-induced proton shift  $-\omega_{\text{Q}}\omega_{\text{D}}/2$  is invariant for the two transitions. This relation allows the determination of relative sign for the dipolar and quadrupolar frequencies. For the spectra in Fig. 1, it was found that for all peak pairs the high frequency  $^{14}\text{N}$  (positive frequency) peak has a lower optimized proton frequency therefore in all cases the product term  $-\omega_{\text{Q}}\omega_{\text{D}}$  is negative. This result indicates that the dipolar and quadrupolar frequencies,  $\omega_{\text{Q}}$  and  $\omega_{\text{D}}$ , should have the same sign. This type of information can be useful to resolve orientation ambiguity in structural refinement

#### 4. Conclusion

It has been shown that  $^{14}\text{N}$ -PISEMA spectra can be acquired for oriented samples with large  $^{14}\text{N}$  quadrupolar coupling similarly as  $^{15}\text{N}$ -PISEMA. Only the  $\sqrt{2}$  scaling factor for the  $^{14}\text{N}$  *rf* nutation frequency and the dipolar-induced proton shift need be considered in setting up the experiment. The spin-lock and exchange are not affected by the large  $^{14}\text{N}$  quadrupolar interaction if the  $^{14}\text{N}$  *rf* field is kept selective to one of the single-quantum transition for a two-level simplification of the spin-1 system. The results from a model compound have demonstrated ultra high  $^{14}\text{N}$  spectral resolution in terms of line width vs. frequency spread while the spectral sensitivity is not suffered from the quadrupolar interactions for oriented samples. The use of  $^{14}\text{N}$  quadrupolar coupling and the enhanced dipolar resolution makes  $^{14}\text{N}$ -PISEMA a potentially useful experiment for oriented membrane peptides and proteins without the requirement of isotope enrichment.

#### Acknowledgments

This work has been supported by the National High Magnetic Field Laboratory through Cooperative Agreement (DMR-0084173) with the National Science Foundation and the State of Florida. C.Q. is grateful for financial support from Bruker Biospin Inc.

#### References

- [1] H.J. Jakobsen, H. Bildsoe, J. Skibsted, T. Giavani, N-14 MAS NMR spectroscopy: the nitrate ion, *J. Am. Chem. Soc.* 123 (2001) 5098–5099.
- [2] T.J. Bastow, D. Massiot, J.P. Coutures, N-14 NMR in AlN and BN, *Solid State Nucl. Magn. Reson.* 10 (1998) 241–245.
- [3] A.K. Khitritin, B.M. Fung, N-14 nuclear magnetic resonance of polycrystalline solids with fast spinning at or very near the magic angle, *J. Chem. Phys.* 111 (1999) 8963–8969.
- [4] E.A. Hill, J.P. Yesinowski, Solid-state N-14 nuclear magnetic resonance techniques for studying slow molecular motions, *J. Chem. Phys.* 107 (1997) 346–354.
- [5] J.S. Santos, D.K. Lee, A. Ramamoorthy, Effects of antidepressants on the conformation of phospholipid headgroups studied by solid-state NMR, *Magn. Reson. Chem.* 42 (2004) 105–114.
- [6] D.J. Siminovitch, M.F. Brown, K.R. Jeffrey, N-14 NMR of lipid bilayers – effects of ions and anesthetics, *Biochemistry* 23 (1984) 2412–2420.
- [7] R. Tycko, S.J. Opella, High-resolution N-14 overtone spectroscopy – an approach to natural abundance nitrogen NMR of oriented and polycrystalline systems, *J. Am. Chem. Soc.* 108 (1986) 3531–3532.
- [8] S. Cavadini, A. Lupulescu, S. Antonijevic, G. Bodenhausen, Nitrogen-14 NMR spectroscopy using residual dipolar splittings in solids, *J. Am. Chem. Soc.* 128 (2006) 7706–7707.
- [9] Z.H. Gan, Measuring amide nitrogen quadrupolar coupling by high-resolution N-14/C-13 NMR correlation under magic-angle spinning, *J. Am. Chem. Soc.* 128 (2006) 6040–6041.
- [10] Z.H. Gan, J.P. Amoureux, J. Trebosc, Proton-detected N-14 MAS NMR using homonuclear decoupled rotary resonance, *Chem. Phys. Lett.* 435 (2007) 163–169.
- [11] S. Cavadini, A. Abraham, G. Bodenhausen, Proton-detected nitrogen-14 NMR by recoupling of heteronuclear dipolar interactions using symmetry-based sequences, *Chem. Phys. Lett.* 445 (2007) 1–5.
- [12] Z.H. Gan, Measuring nitrogen quadrupolar coupling with C-13 detected wide-line N-14 NMR under magic-angle spinning, *Chem. Commun.* (2008) 868–870.
- [13] A. Ramamoorthy, L.M. Gierasch, S.J. Opella, Three-dimensional solid-state NMR correlation experiment with  $^1\text{H}$  homonuclear spin exchange, *J. Magn. Reson. B* 111 (1996) 81–84.
- [14] C.H. Wu, S.J. Opella, Proton-detected separated local field spectroscopy, *J. Magn. Reson.* 190 (2008) 165–170.
- [15] C.H. Wu, A. Ramamoorthy, S.J. Opella, High-resolution heteronuclear dipolar solid-state NMR Spectroscopy, *J. Magn. Reson.* 109 (1994) 270.
- [16] R. Tycko, P.L. Stewart, S.J. Opella, Peptide plane orientations determined by fundamental and overtone N-14 NMR, *J. Am. Chem. Soc.* 108 (1986) 5419–5425.
- [17] R.K. Hester, J.L. Ackerman, B.L. Neff, J.S. Waugh, Separated local field spectra in NMR – determination of structure of solids, *Phys. Rev. Lett.* 36 (1976) 1081–1083.
- [18] J.R. Lewandowski, G. De Paepe, R.G. Griffin, Proton assisted insensitive nuclei cross polarization, *J. Am. Chem. Soc.* 129 (2007) 728–729.
- [19] Z. Gan, Spin dynamics of polarization inversion spin exchange at the magic angle in multiple spin systems, *J. Magn. Reson.* 143 (2000) 136–143.
- [20] R. Mcnamara, C.H. Wu, L.E. Chirlian, S.J. Opella, Direct observation of asymmetric H-1/N-14 triplets and applications of asymmetric dipole–dipole splittings to structure determination by solid-state NMR-spectroscopy, *J. Am. Chem. Soc.* 117 (1995) 7805–7811.
- [21] P.L. Gor'kov, E.Y. Chekmenev, C.G. Li, M. Cotten, J.J. Buffy, N.J. Traaseth, G. Veglia, W.W. Brey, Using low-E resonators to reduce RF heating in biological samples for static solid-state NMR up to 900 MHz, *J. Magn. Reson.* 185 (2007) 77–93.
- [22] A.O. Jardetzky, G.C.K. Roberts, *NMR in Molecular Biology*, Academic Press, New York, 1981.
- [23] J.R. Quine, T.A. Cross, Protein structure in anisotropic environments: unique structural fold from orientational constraints, *Concept. Magn. Reson.* 12 (2000) 71–82.